Geophysical Research Letters

RESEARCH LETTER
10.1029/2024GL108271

Deglacial Pulse of Neutralized Carbon From the Pacific Seafloor: A Natural Analog for Ocean Alkalinity Enhancement?

R. A. Green[1], M. P. Hain[1], and P. A. Rafter[2]

[1]Earth and Planetary Science Department, University of Santa Cruz, Santa Cruz, CA, USA, [2]College of Marine Science, University of South Florida, St. Petersburg, FL, USA

Key Points:

- Observed deglacial changes in atmospheric CO_2 and $^{14}C/C$ allow for up to 2,396 Pg of neutralized geologic carbon (i.e., bicarbonate) release
- The global carbon cycle is essentially "blind" to neutralized carbon release, only constrained by ^{14}C budget
- This gigaton-scale neutralized carbon release may be a natural analog to the marine CO_2 removal method of ocean alkalinity enhancement

Supporting Information:

Supporting Information may be found in the online version of this article.

Correspondence to:

R. A. Green,
rygreen@ucsc.edu

Citation:

Green, R. A., Hain, M. P., & Rafter, P. A. (2024). Deglacial pulse of neutralized carbon from the Pacific seafloor: A natural analog for ocean alkalinity enhancement? *Geophysical Research Letters*, *51*, e2024GL108271. https://doi.org/10.1029/2024GL108271

Received 17 JAN 2024
Accepted 1 MAR 2024

Author Contributions:

Conceptualization: M. P. Hain, P. A. Rafter
Formal analysis: R. A. Green
Funding acquisition: M. P. Hain, P. A. Rafter
Methodology: R. A. Green, M. P. Hain, P. A. Rafter
Project administration: M. P. Hain, P. A. Rafter
Software: R. A. Green
Supervision: M. P. Hain, P. A. Rafter
Visualization: R. A. Green
Writing – original draft: R. A. Green
Writing – review & editing: R. A. Green, M. P. Hain, P. A. Rafter

Abstract The ocean carbon reservoir controls atmospheric carbon dioxide (CO_2) on millennial timescales. Radiocarbon (^{14}C) anomalies in eastern North Pacific sediments suggest a significant release of geologic ^{14}C-free carbon at the end of the last ice age but without evidence of ocean acidification. Using inverse carbon cycle modeling optimized with reconstructed atmospheric CO_2 and $^{14}C/C$, we develop first-order constraints on geologic carbon and alkalinity release over the last 17.5 thousand years. We construct scenarios allowing the release of 850–2,400 Pg C, with a maximum release rate of 1.3 Pg C yr^{-1}, all of which require an approximate equimolar alkalinity release. These neutralized carbon addition scenarios have minimal impacts on the simulated marine carbon cycle and atmospheric CO_2, thereby demonstrating safe and effective ocean carbon storage. This deglacial phenomenon could serve as a natural analog to the successful implementation of gigaton-scale ocean alkalinity enhancement, a promising marine carbon dioxide removal method.

Plain Language Summary The ocean is the largest carbon reservoir on Earth's surface and, as such, it controls the concentration of the greenhouse gas carbon dioxide (CO_2) in the atmosphere over long time periods. When CO_2 was rising at the end of the last ice age, marine sediment evidence indicates a regional carbon release into the ocean, due to a distinct carbon isotope fingerprint left behind. Using a carbon cycle model and atmospheric data, we simulated different geologic carbon addition scenarios since the last ice age. We find that substantial carbon addition to the ocean could have occurred (up to 1.3 billion tons per year) without causing significant changes to the carbon cycle, but only if the carbon is neutralized by alkalinity in an approximate 1:1 ratio. This neutralized release is similar to an approach of carbon removal called ocean alkalinity enhancement (OAE), which aims to reduce atmospheric CO_2 as a potential solution for climate change. These findings suggest that neutralized carbon addition—in the form of "neutralized" bicarbonate ion $\left(HCO_3^-\right)$ instead of "acidic" CO_2—could explain the low levels of radiocarbon during the last deglaciation and shows that large-scale OAE is feasible without causing major changes to the marine carbon cycle.

1. Introduction

Global climate, the global carbon cycle, and the atmospheric concentration of the greenhouse gas carbon dioxide (CO_2) have been tightly coupled over recent ice age cycles (Siegenthaler et al., 2005), including the relatively abrupt ice age terminations and deglacial periods (Marcott et al., 2014; Shakun et al., 2012). Coupled changes in deep ocean circulation, polar ocean biological nutrient consumption, and air-sea CO_2 exchange are thought to be the dominant drivers of the observed CO_2 change (Khatiwala et al., 2019; Rafter et al., 2022; Sigman et al., 2021), but changes in land carbon storage and seafloor carbon burial in direct response to climate change are also clearly implicated (Cartapanis et al., 2018; Joos et al., 2001; Köhler et al., 2014). The primary challenge to all these hypotheses comes from unexplained "anomalies" in the radiocarbon (^{14}C) content within marine foraminifera during deglacial CO_2 rise in the atmosphere, between about 18,000 and 11,500 years before 1950 (18–11.5 thousand years before present or kyr BP, Figure 1). These deglacial records of ^{14}C depletion (decay-corrected ^{14}C:^{12}C ratio, expressed as $\Delta^{14}C$; Stuiver & Polach, 1977) have been uncovered throughout the intermediate-depth (>500 m & <1,000 m) eastern tropical North Pacific (ETNP) Ocean (Lindsay et al., 2016; Marchitto et al., 2007; Rafter et al., 2018, 2019; Stott et al., 2009); associated with the weakly ventilated Pacific shadow zone (Gehrie et al., 2006; Holzer et al., 2021).

These regional depletions in seawater $\Delta^{14}C$ were initially attributed to a release of dissolved inorganic carbon (DIC) that had been sequestered for thousands of years in the abyssal ocean, hinting at deglacial changes in ocean

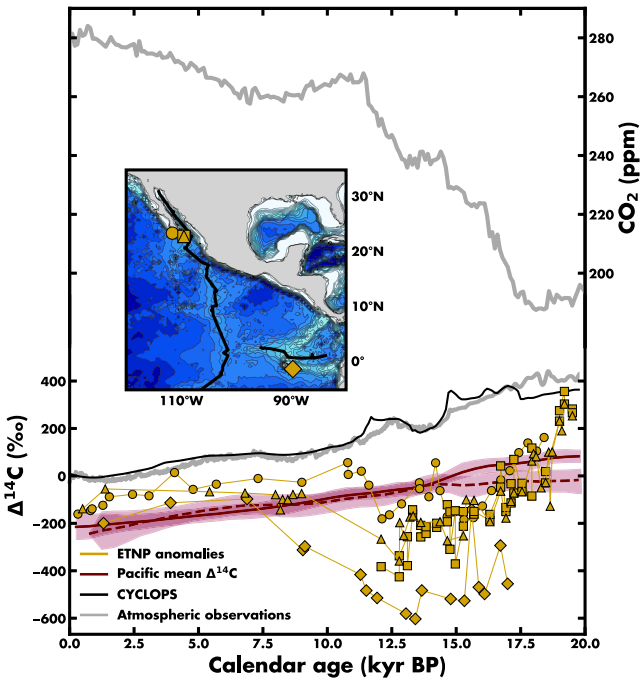

Figure 1. Unexplained $\Delta^{14}C$ anomalies from the intermediate-depth (>500 m and <1,000 m) eastern tropical North Pacific (ETNP). The ETNP anomalies shown are foraminifera from Marchitto et al. (2007) (benthic; circles), Stott et al. (2009) (benthic; diamonds), and Rafter et al. (2018) (squares for benthic, triangles for planktic). The ETNP anomalies are compared with compilation means from the Pacific (red lines; Rafter et al., 2022). Solid and dashed lines represent mid-depth and bottom water, respectively, with red shading denoting the 95% confidence interval. The atmospheric $\Delta^{14}C$ for our CYCLOPS control simulation is shown as a solid black line. Reconstructed atmospheric $\Delta^{14}C$ (Reimer et al., 2020) and CO_2 (Bereiter et al., 2015) are shown in gray. Individual $\Delta^{14}C$ records are overlaid on ocean bathymetry (blue contours) and tectonic spreading centers (black lines) in the map inset.

circulation (Bova et al., 2018; Broecker, 2009; Broecker & Barker, 2007; Marchitto et al., 2007). However, this ocean release interpretation has two main shortcomings (Hain et al., 2011): (a) the Last Glacial Maximum (LGM) deep ocean was not sufficiently ^{14}C-depleted (dashed red line in Figure 1) to be the source of the mid-depth anomalies, and (b) once the isotopic signature of anomalously ^{14}C-depleted carbon is transported to the mid-depth Pacific it would rapidly dissipate into the global carbon cycle via ocean circulation and air-sea gas exchange. This hypothesis is further contradicted by a new compilation showing no appreciable ^{14}C-depletion at any depth for the basin-scale Pacific during the deglaciation (red lines in Figure 1; Rafter et al., 2022), as would be required if the abyssal ocean caused the ETNP ^{14}C anomalies. Additionally, deep-sea coral ^{14}C records from the Galápagos with excellent age model controls (Chen et al., 2020) and South Pacific ^{14}C records bathed in modern Antarctic Intermediate Water (De Pol-Holz et al., 2010; Rose et al., 2010; Siani et al., 2013; Zhao & Keigwin, 2018) show no ^{14}C-depletion comparable to the ETNP anomalies. This lack of basin-wide mid-depth $\Delta^{14}C$ depletion is an important observational constraint we will consider below.

An alternative set of proposals suggests these anomalously low $\Delta^{14}C$ values reflect an addition of ^{14}C-free carbon from a geologic source (Rafter et al., 2018, 2019; Ronge et al., 2016; Skinner & Bard, 2022; Stott et al., 2009; Stott & Timmermann, 2011). A common objection to this hypothesis is the potential for ocean acidification, which would contradict the evidence of ETNP carbonate preservation during the last deglacial (Lindsay et al., 2015; Marchitto et al., 2007; Ortiz et al., 2004; Rafter et al., 2019; Skinner & Bard, 2022; Stott et al., 2009). However, if a proportional influx of alkalinity neutralized the geologic carbon—e.g., carbon introduced in the form of "neutralized" bicarbonate ion instead of "acidic" CO_2—there would be muted effects on seawater pH, $CaCO_3$ burial, and atmospheric CO_2 (Rafter et al., 2019).

Neutralized ^{14}C-free carbon could be generated within marine sediments via metamorphic or hydrothermal processes (Rafter et al., 2019; Skinner & Bard, 2022). Subsequently, it would be transported and dispersed throughout the ocean and atmosphere, leading to the dilution of the atmospheric ^{14}C reservoir and a reduction of atmospheric $\Delta^{14}C$. While the majority of the atmospheric $\Delta^{14}C$ decline during the last deglaciation has been attributed to Southern Ocean CO_2 release, changes in Atlantic circulation, and a decline in cosmogenic ^{14}C production due to a strengthening of Earth's magnetic field (black line in Figure 1; Hain et al., 2014; Skinner & Bard, 2022), these processes alone do not fully account for changes observed in reconstructed atmospheric $\Delta^{14}C$ records (Reimer et al., 2020). This discrepancy indicates a possible opportunity within the planetary ^{14}C budget for ^{14}C-free geologic carbon addition.

This study presents the first carbon cycle model results investigating the possibility of coupled geologic carbon and alkalinity release during the last deglaciation. Our experiments build on the deglacial model scenario of Hain et al. (2014) and test the sensitivity of our results to changes in terrestrial carbon storage. We use a stepwise numerical model optimization method that assimilates observed atmospheric CO_2 and $\Delta^{14}C$ data to find the internally consistent rates of geologic carbon and alkalinity release, permafrost carbon destabilization, and land biosphere regrowth. This is intended to raise important questions relevant to different fields of research: can seafloor spreading centers respond to climate change? What subsurface processes could mobilize carbon and alkalinity at relevant specific rates? And do deglacial radiocarbon anomalies provide a natural analog for purposeful ocean alkalinity enhancement (OAE) as a means of marine carbon dioxide removal (Bach & Boyd, 2021; NASEM, 2021)?

2. Materials and Methods

Motivated by the regional ETNP anomalies (Figure 1), we use the CYCLOPS global carbon cycle model (Hain et al., 2010, 2011, 2014; Keir, 1988; see Text S1 in Supporting Information S1 for model configuration) to simulate the flux of geologic carbon from Pacific mid-ocean ridge systems. This involves four experiments, progressively adding optimized open-system carbon and alkalinity fluxes, along with an imposed initial ^{14}C inventory change (top row of Figure 2): (a) We invert for the optimal rates of carbon and alkalinity release to the intermediate-depth (200–1500m) North Pacific region of the model (experiment NP); (b) We add the possibility of land carbon uptake to the optimization (experiment NP + LC); (c) We include the release of ^{14}C-free permafrost carbon to the atmosphere (experiment NP + LC + PF); and (d) We adjust the initial LGM ^{14}C inventory by +3.5% to account for the uncertain history of Earth's magnetic field, ^{14}C production, and reconstructed $\Delta^{14}C$ near the LGM (Figure 3a, Dinauer et al., 2020; Roth & Joos, 2013) (experiment NP + LC + PF + RC).

All experiments include the identical background forcings of the control run, based on the deglacial carbon cycle scenario from Hain et al. (2014). Although this is an idealized model scenario, we use it as our starting point because the LGM carbon cycle forcing of CYCLOPS is well documented (Hain et al., 2010) and consistent with reconstructed surface ocean pH changes (Chalk et al., 2017; Hain et al., 2018). Additionally, the deglacial model scenario agrees reasonably well with subsequent ^{14}C measurements and data compilations (Rafter et al., 2022; Zhao et al., 2018), as shown by the direct comparison for the Pacific and all other basins (Figure S1 in Supporting Information S1). More in-depth descriptions of each experiment can be found in Text S3 of Supporting Information S1.

For all experiments, the optimized open-system carbon and alkalinity fluxes were determined by a numerical algorithm that minimizes the deviation between simulated atmospheric CO_2 (CO_2^{model}) and $\Delta^{14}C$ ($\Delta^{14}C^{model}$), compared to reconstructed atmospheric CO_2 (CO_2^{obs}) from the most recent compilation of Antarctic ice core CO_2 data (Bereiter et al., 2015) and $\Delta^{14}C$ ($\Delta^{14}C^{obs}$) from IntCal20 (Reimer et al., 2020). The algorithm's objective function f is scaled to the 90ppm glacial/interglacial CO_2 range and the ~250‰ atmospheric $\Delta^{14}C$ change after accounting for Earth's magnetic field strengthening:

$$f(CO_2, \Delta^{14}C) = \frac{\left|CO_2^{obs} - CO_2^{model}\right|}{90\ ppm} + \frac{\left|\Delta^{14}C^{obs} - \Delta^{14}C^{model}\right|}{250\ ‰}$$

We do not permit unrealistic 'negative' geologic fluxes, permafrost growth, or land carbon contraction that could otherwise help the model align with the observations. For experiments that include land carbon uptake, we included a deliberate heuristic favoring land carbon uptake during the Holocene. If CO_2^{model} was greater than CO_2^{obs} and the atmospheric $\Delta^{14}C$ model-data misfit was less than 20‰, then the optimized carbon flux is added to the terrestrial biosphere rather than the intermediate-depth North Pacific (with an alkalinity flux of zero). For experiments that include carbon release from permafrost destabilization, the optimized flux is only activated when the optimization algorithm would otherwise add CO_2 (ALK-to-DIC<0.5) into the intermediate-depth North Pacific, instead releasing the equivalent amount of CO_2 directly to the atmosphere. Further algorithm details can be found in Text S2 of Supporting Information S1.

3. Results

3.1. Atmospheric Constraints on Geologic Carbon Addition

All four simulations improve the overall CO_2 and $\Delta^{14}C$ model-data misfit compared to the control run (blue vs. black line, Figure 2). This model-data misfit is progressively minimized as more open-system carbon and alkalinity fluxes are added, with the NP + LC + PF + RC simulating the smallest model-data misfit. Each simulation has two main pulses of geologic carbon, one during the deglaciation and one smaller pulse during the Holocene. Our optimization triggers these geologic pulses when $\Delta^{14}C^{model}$ rises above $\Delta^{14}C^{obs}$, which we call ^{14}C opportunities. Most geologic carbon is added as bicarbonate ion (61%–84%, Table S1 in Supporting Information S1), with net ALK-to-DIC ratios between 1.08 and 1.19 (Table S1 in Supporting Information S1) across all four simulations.

For our first three experiments (NP, NP + LC, NP + LC + PF)–which include no adjustment to the initial ^{14}C inventory–a total of 846–929 Pg C geologic carbon was added over the 20-kyrs (Table S1 in Supporting

10.1029/2024GL108271

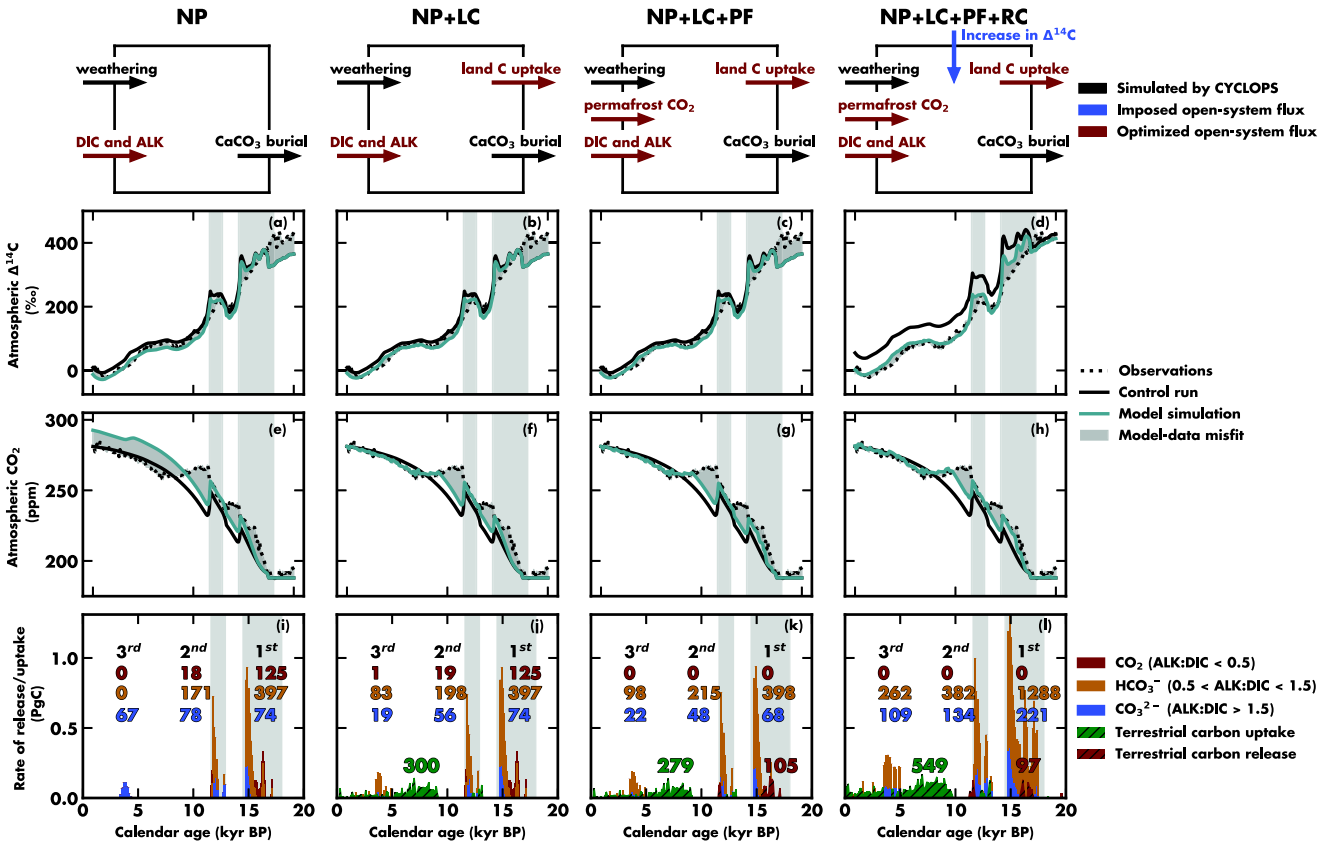

Figure 2. Simulated atmospheric response to optimized geologic carbon release scenarios. The top row illustrates our experimental design that progressively introduces optimized and imposed open-system fluxes (colored arrows). Subsequent rows illustrate simulation results for atmospheric $\Delta^{14}C$ (a–d), atmospheric CO_2 (e–h), and carbon release/uptake rates (i–l). In panels (i–l), colored numbers represent the amounts of CO_2 (red), HCO_3^- (yellow), and CO_3^{2-} (blue) released with each geologic carbon pulse. Similarly, terrestrial carbon uptake (regrowth) is shown in green, and terrestrial carbon release (permafrost destabilization) is in red, all in units of Pg C. Gray bars denote Heinrich Stadial 1 and Younger Dryas, while model-data misfit is shaded in gray.

Information S1), with peak rates as large as 0.9 Pg C yr^{-1} (Figures 2i–2k) during the first pulse of addition (~15-kyr BP). Of those experiments that included terrestrial regrowth (NP + LC, NP + LC + PF), simulated carbon uptake is between 279 and 300 Pg C (Table S1 in Supporting Information S1), mainly during the Holocene. When we include terrestrial carbon release from permafrost thaw (NP + LC + PF), 105 Pg C (Figure 2k, Table S1 in Supporting Information S1) is released around 16-kyr BP during the first pulse of carbon addition. Our fourth experiment, NP + LC + PF + RC, includes an adjusted ^{14}C inventory at the LGM initial state alongside all the above open-system fluxes. The higher initial $\Delta^{14}C^{model}$ increases the opportunity for the subsequent addition of ^{14}C-free carbon, leading to a greater amount of total carbon added (2,396 Pg C, Table S1 in Supporting Information S1), higher release rates (up to 1.3 Pg C yr^{-1}, Figure 2l), more land carbon uptake (550 Pg C; Table S1 in Supporting Information S1), but a similar carbon release from permafrost thaw around 16-kyr BP (97 Pg C).

3.2. Regional and Bulk Ocean Impacts From Large-Scale Geologic Carbon Addition

The most severe carbon cycle impacts should arise during our largest geologic carbon addition scenario (NP + LC + PF + RC). However, only minor $\Delta^{14}C$ anomalies are simulated in the intermediate-depth North Pacific box where the carbon is released (solid blue line, Figure 3a). Consequently, the simulated intermediate-depth North Pacific $\Delta^{14}C$ is in broad agreement with the mean $\Delta^{14}C$ from the mid-depth (neutral density of 27.5–28 kg m^{-3}) Pacific, calculated from a new proxy $^{14}C/C$ compilation (red line in Figure 3a and Rafter et al., 2022). Given that the present-day mid-depth Pacific contains the oldest waters in the ocean, it serves as a conservative benchmark for comparing our simulated intermediate-depth results. Furthermore, the lack of severe $\Delta^{14}C$ depletion in the

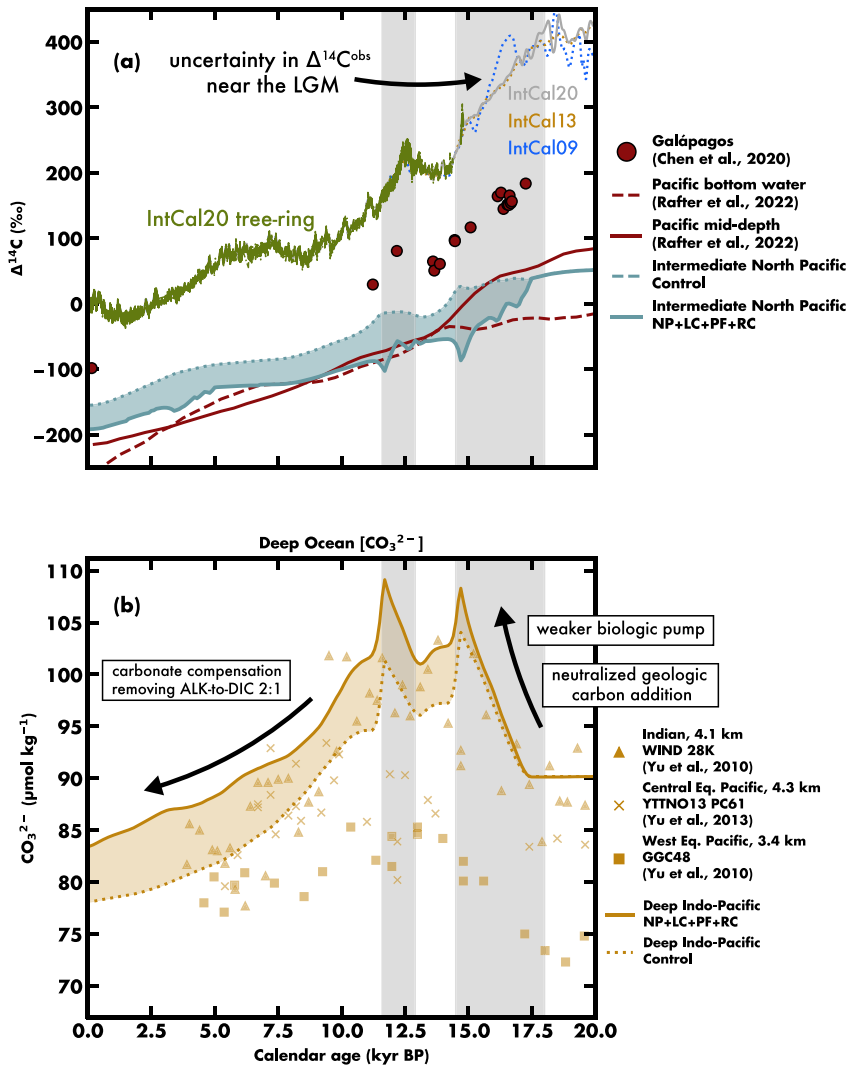

Figure 3. Neutralized carbon release has limited impacts on basin scale $\Delta^{14}C$ and deep ocean $\left[CO_3^{2-}\right]$. In Panel a, NP + LC + PF + RC drives mild $\Delta^{14}C$ depletion from the control run (shaded blue area), consistent with various data sets: deep-sea coral near the Galápagos (red circles), mean $\Delta^{14}C$ from Pacific mid-depth and bottom water (solid and dashed red line), and atmospheric $\Delta^{14}C$ (solid gray and green, dotted yellow and blue). There is a notable discrepancy in $\Delta^{14}C$ near the Last Glacial Maximum in the last three IntCal iterations before converging when tree-ring data becomes available (solid green line). Panel b illustrates NP + LC + PF + RC causing an increase in $[CO_3^{2-}]$ in the Indo-Pacific deep ocean compared to the control run (shaded yellow). Simulated $\left[CO_3^{2-}\right]$ align broadly with observations from the Indian (yellow triangle) and Equatorial Pacific (yellow square and X). Gray bars represent Heinrich Stadial 1 and Younger Dryas.

NP + LC + PF + RC simulation is supported by a deep-sea coral record considered representative of the ^{14}C content of intermediate waters near the Galápagos islands (red circles in Figure 3a and Chen et al., 2020).

Similarly, we find limited impacts on deep ocean $\left[CO_3^{2-}\right]$–which largely determines $CaCO_3$ saturation and thus $CaCO_3$ burial–when the geologic carbon is added as HCO_3^- (ALK-to-DIC ~ 1). This is clear from Figure 3b and as the NP + LC + PF + RC only simulates a moderate increase (~5 μmol kg^{-1}) in deep-ocean $\left[CO_3^{2-}\right]$ compared to the control simulation. With a deglacial increase in deep-ocean $\left[CO_3^{2-}\right]$ due to a weakened biological pump and a subsequent decrease in deep-ocean $\left[CO_3^{2-}\right]$ from carbonate compensation, both the control and NP + LC + PF + RC simulation broadly follow $\left[CO_3^{2-}\right]$ observations (Yu et al., 2010, 2013).

In addition to $\Delta^{14}C$ impacts, geologic carbon will impact the ocean's stable isotope ratio of carbon ($^{13}C/^{12}C$, reported as $\delta^{13}C$), but this ultimately depends on the source. We run an additional set of experiments by

calculating the bulk ocean $\delta^{13}C$ change for two endmember sources of neutralized geologic carbon (described in Text S4 of Supporting Information S1): bicarbonate from anaerobic oxidation of thermogenic methane (AOM; Rafter et al., 2019) and geologic CO_2 neutralized by carbonate dissolution (Skinner & Bard, 2022), with $\delta^{13}C$ values of −25‰ and −2.5‰, respectively. When 2,396 Pg C is added (as suggested by our NP + LC + PF + RC experiment), we simulate bulk $\delta^{13}C$ ocean changes of −1.5‰ for AOM and −0.2‰ for carbonate dissolution. Given that reconstructed oceanic $\delta^{13}C$ values have not fluctuated more than ∼1‰ over the last 800-kyrs (Hodell et al., 2003), our simulations suggest geologic carbon from a methane source ($\delta^{13}C \leq -25‰$) is unlikely for our extreme carbon addition scenario of 2,396 Pg C. Considering the decoupled nature of neutralized geologic carbon addition and atmospheric CO_2, along with the limited impact on basin-scale $\Delta^{14}C$, deep ocean $\left[CO_3^{2-}\right]$, and bulk ocean $\delta^{13}C$, these findings underscore that the global ^{14}C budget is the strongest constraint available for assessing geologic carbon addition at the global scale.

4. Discussion

The core outcome of our study is that atmospheric CO_2 and $CaCO_3$ burial are effectively blind to carbon release neutralized by alkalinity in a ratio near 1:1, with the timely implication that OAE may be an effective pathway for the mitigation of anthropogenic carbon emissions (NASEM, 2021). In the specific context of the deglacial period, this insensitivity allows for large-scale geologic carbon addition scenarios constrained most directly by the planetary radiocarbon budget, as long as there was concomitant natural OAE. Additionally, our most extreme carbon addition scenario is insufficient to drive significant $\Delta^{14}C$ depletion across the North Pacific, which agrees with observations representative of the North Pacific and Pacific basins. This supports the idea that the enigmatic $\Delta^{14}C$ anomalies of the ETNP are likely regional or localized phenomena that could be exploited to derive a set of local constraints on possible carbon and alkalinity release that would be completely independent of the global CO_2 and ^{14}C budget constraints used in this study.

4.1. Large Amounts of Bicarbonate Allowable

We optimized our carbon cycle modeling simulations, which include different open-system fluxes and changes to the ^{14}C inventory, with the addition of geologic carbon. The simulations show that up to 2,396 Pg of geologic carbon, mainly as bicarbonate ion, can be consistent with the observed deglacial changes in atmospheric CO_2 and $\Delta^{14}C$. Due to the alkalinity accompanying DIC during bicarbonate addition, geologic carbon in this form can be added at rates as large as 1.3 Pg C yr^{-1} (Figure 2l) with limited impacts on atmospheric CO_2 and deep-sea $\left[CO_3^{2-}\right]$.

Prior work has estimated that deglacial geologic CO_2 emissions from mantle decompression could have reached up to 0.2 Pg C yr^{-1} (Cartapanis et al., 2018; Roth & Joos, 2012), much smaller than our maximum yearly rates. However, these lower rates were derived assuming the geologic carbon came only as CO_2 rather than as bicarbonate ion. When carbon is added without alkalinity (i.e., CO_2), atmospheric CO_2 and $CaCO_3$ burial constraints are highly sensitive to any carbon added to the system. However, when adding neutralized carbon (bicarbonate), atmospheric CO_2 and $CaCO_3$ burial constraints become effectively blind to the carbon release, no longer constraining the carbon release rate or total. During bicarbonate addition, the constraining factor shifts to the planetary ^{14}C mass balance and its reflection in the atmospheric $\Delta^{14}C$ record (via IntCal20, Reimer et al., 2020), which can indirectly record the dilution of ^{14}C-enriched environmental carbon by ^{14}C-free geologic carbon. This $\Delta^{14}C^{obs}$ constraint on bicarbonate release leads to an upper bound of 800–1,000 Pg C in our first three simulations (NP, NP + LC, NP + LC + PF)—a 2%–2.5% increase of total ocean carbon inventory. Furthermore, if we take into consideration the uncertainty in the planetary ^{14}C mass balance (Dinauer et al., 2020; Roth & Joos, 2013) by increasing the initial LGM ^{14}C inventory by 3.5%, the opportunity for subsequent geologic carbon release increases to ∼2,500 Pg C (6.5% increase of total ocean carbon inventory). In other words, a higher initial LGM ^{14}C/C can substantially increase the opportunity for ^{14}C-free geologic carbon release since the LGM.

Considering the idealized nature of our experiments and because of biases inherited from our control run (Hain et al., 2014), our optimization results should not be taken as estimates of geologic carbon release or of other simulated open-system carbon fluxes (e.g., LC, PF). Instead, we argue that geologic carbon release greater than 800–1000 Pg C is rendered unlikely, and release greater than 2,400 Pg C is implausible in the face of $\Delta^{14}C^{obs}$. Further, if indeed there was substantial geologic carbon release since the LGM, it must have been in the neutralized form of bicarbonate ion with a net ALK-to-DIC ratio near 1, as proposed by Rafter et al. (2019), to

avoid violating constraints from atmospheric CO_2 and $CaCO_3$ burial. Therefore, we argue that geologic carbon release played only a minor role in raising CO_2 at the end of the last ice age, even if the total amount of carbon release was substantial. This contrasts with prior deglacial geologic carbon addition research, which attributes glacial/interglacial CO_2 variability to liquid CO_2 release (Stott, Davy, et al., 2019; Stott, Harazin, & Krupinski, 2019; Stott & Timmermann, 2011).

4.2. Geologic Carbon as an Explanation for $\Delta^{14}C$ Anomalies?

When first discovered, the $\Delta^{14}C$ anomalies in the ETNP were taken to be the signature of carbon release from the deep ocean to the atmosphere (Marchitto et al., 2007). This earlier view of the $\Delta^{14}C$ anomalies buttresses the longstanding notion that stagnation of deep ocean circulation during the LGM created an isolated ^{14}C-deplete reservoir for the sequestration of atmospheric CO_2 (Broecker & Barker, 2007; Skinner et al., 2010)—and this view remains prevalent (e.g., Bova et al., 2018). However, deep ocean carbon storage and its effect on atmospheric CO_2 is more closely tied to the degree of nutrient consumption in the polar ocean regions that form new deep water (Hain et al., 2010, 2014; Ito & Follows, 2005; Marinov, Follows, et al., 2008; Marinov, Gnanadesikan, et al., 2008b; Sigman et al., 2010, 2021; Sigman & Haug, 2003) rather than being a simple function of the rate of deep ocean overturning. Further, a new compilation of global ocean $\Delta^{14}C$ records reveals that the LGM ^{14}C age of the global deep ocean was about ~1,000 years greater than today (Rafter et al., 2022), sufficient to explain a large portion of the observed $\Delta^{14}C^{obs}$ decline during the deglacial period (Broecker & Barker, 2007; Hain et al., 2014), but not nearly ^{14}C-deplete enough to produce the ETNP $\Delta^{14}C$ anomalies (Figure 3a). Rather than becoming a plank in our evolving understanding of coupled glacial/interglacial changes in ocean circulation and the global carbon cycle, the existence of these $\Delta^{14}C$ anomalies has become its own vexing problem, defying conventional explanations based on ocean circulation.

There are numerous reasons why a given sample would yield an anomalously low reconstructed $^{14}C/C$, but the spatial-temporal clustering of ^{14}C anomalies in the upper 1 km of the ETNP water column is remarkable (e.g., Bova et al., 2018; Lindsay et al., 2015; Marchitto et al., 2007; Rafter et al., 2018, 2019; Stott, Davy, et al., 2019; Stott, Harazin, & Krupinski, 2019), especially when contrasted with nearby records that broadly track atmospheric ^{14}C change without discernible ^{14}C anomalies (e.g., Bova et al., 2018; Chen et al., 2020; De Pol-Holz et al., 2010; Rose et al., 2010; Siani et al., 2013; Zhao & Keigwin, 2018). Previous modeling of the problem suggests that any ^{14}C anomaly in the upper ocean would rapidly dissipate by ocean circulation and air-sea gas exchange (Hain et al., 2011) such that upper ocean $\Delta^{14}C$ is expected to track atmospheric $\Delta^{14}C$ change since the LGM (Hain et al., 2014), as is observed in independently dated coral ^{14}C records from the Atlantic and Pacific (e.g., Chen et al., 2020) and other records outside the anomalous ETNP cluster. Our new results advance the argument by demonstrating that even the release of >2,000 Pg C is insufficient to generate a significant ^{14}C anomaly on the basin scale resolved in our current model (Figure 3a), related to the rapid global dissipation of ^{14}C isotope anomalies in the global carbon cycle (Hain et al., 2011). That is, the absence of anomalies in most upper ocean ^{14}C reconstructions is normal and expected, even in the case of substantial simulated carbon release. The caveat to the argument is that a small $\Delta^{14}C$ reduction simulated at the basin scale would be consistent with a severe ^{14}C anomaly concentrated in a small sub-region, such as observed in the ETNP.

The ^{14}C anomalies of the ETNP may record carbon release associated with processes linked to spreading centers separating the Cocos, Nazca, and Pacific plates that produce very high regional geothermal heat flux (>0.1 W m^{-2} throughout the region; Pollack et al., 1993). While we cannot usefully comment on whether these geologic systems are dynamic enough to yield defined pulses of carbon release, our results highlight that only a neutralized form of carbon release would be consistent with the atmospheric CO_2 constraint and observations of good (sometimes improved) seafloor carbonate preservation (Figure 3b; Yu et al., 2008, 2010, 2013) during the main purported geologic carbon pulses. Indeed, the temporal coincidence of the ^{14}C anomalies with stadial/interstadial climate change, deglacial ocean heat uptake (Poggemann et al., 2018), and circulation change (e.g., McManus et al., 2004; Rafter et al., 2022) may point to a climatic or environmental trigger of carbon release, rather than a being a purely stochastic volcanogenic phenomenon.

However, why would severe ^{14}C anomalies persist for millennia in the ETNP upper ocean water column if ocean circulation and air-sea gas exchange act to rapidly dissipate the anomalous carbon globally (Hain et al., 2011)? We propose two alternative resolutions that we cannot distinguish based on our current model and existing data: Either the anomalies are localized and reflect geologic carbon diffusion out of the underlying sediment stack rather than

bottom water $\Delta^{14}C$, or the anomalies are regional and reflect the accumulation of geologic carbon in the ETNP shadow zone of ocean circulation with a sharp and persistent chemical gradient to the open ocean mid-depth Pacific.

If the anomalies are localized, we might expect each anomalous record to differ in magnitude and timing. Finding individual mid-depth sites in the ETNP where ^{14}C anomalies are missing (e.g., Bova et al., 2018; Chen et al., 2020) alongside records with ^{14}C anomalies that are only broadly similar would tend to support the localized explanation. Conversely, if geologic carbon were added to a dynamically isolated region, such as the upper ocean ETNP (Margolskee et al., 2019), seawater $\Delta^{14}C$ might diverge substantially from the $\Delta^{14}C$ of the open Pacific and atmosphere. However, that regional signal would need to be shared by all radiocarbon records in the hydrodynamic region (cf. Chen et al., 2020). If the anomalies did reflect the restricted regional ocean circulation of the ETNP, it would seem plausible that the carbon release mechanism also operated in regions outside the ETNP (e.g., Bryan et al., 2010).

5. Conclusion

We document a set of carbon cycle model scenarios since the LGM that include substantial (800–2,400 Pg C) release of geologic carbon broadly consistent with reconstructed atmospheric CO_2 rise, $\Delta^{14}C$ decline, and $CaCO_3$ burial patterns. In all simulations, geologic carbon release is primarily released as bicarbonate ion (i.e., with an ALK-to-DIC near 1), with minimal effect on the marine carbon cycle and atmospheric CO_2. That is, we demonstrate the possibility of climate-neutral geologic carbon and alkalinity release during the deglacial period in a way that is consistent with a dominant Southern Ocean control on climate-carbon coupling over ice age cycles. As such, we do not prove that such geologic carbon release happened, but rather we hope to expand what is deemed possible. The central outcome of this study is that the deglacial $\Delta^{14}C$ anomalies from the ETNP region may represent a natural analog for the successful application of OAE as a means to neutralize anthropogenic carbon emissions.

Introducing geologic carbon will dilute the planetary inventory of cosmogenic radiocarbon (^{14}C) such that the largest release of ^{14}C-free carbon (2,400 Pg C) can reduce the average $\Delta^{14}C$ of environmental carbon by about ~50‰. Therefore, the planetary ^{14}C budget can be used to rule out the most extreme scenarios for geologic carbon release, offering an upper-bound constraint for carbon transfers from geologic and terrestrial carbon reservoirs to the ocean/atmosphere carbon cycle. That is, our model scenarios are designed to explore the limit of what appears to be possible in the context of global constraints from CO_2 and ^{14}C reconstructions. We find that bicarbonate release was likely limited to less than 1,000 Pg C, but when considering uncertainty in the history of cosmogenic ^{14}C production, the limit for bicarbonate release may be as high as 2,400 Pg C.

The spatial cluster of deglacial $\Delta^{14}C$ anomalies in the upper water column of the ETNP may be evidence for geologic carbon release associated with the seafloor spreading center defining the East Pacific Rise (Figure 1; Lindsay et al., 2015; Marchitto et al., 2007; Rafter et al., 2018, 2019; Stott et al., 2009). Confirming or rejecting this hypothesis would have several implications: Without large-scale carbon release, we lack an adequate explanation for the ETNP $\Delta^{14}C$ anomalies, suggesting an open gap in our understanding of the ^{14}C-proxy system used to reconstruct ocean circulation changes in response to deglacial climate change. Alternatively, with large pulses of geologic carbon release in the ETNP, we lack an adequate explanation for how bicarbonate is derived from geologic carbon sources during the deglaciation, suggesting a gap in our understanding of glacial/interglacial changes in seafloor spreading and its role in the global carbon cycle.

Data Availability Statement

Detailed model description and configuration are available in the Supporting Information. The plotting code and simulation results are found on GitHub (https://github.com/RyanAGreen/Deglacial-Neutralized-Carbon-14C) and Zenodo (https://zenodo.org/badge/latestdoi/627637425; Green, 2023).

Acknowledgments
This research was funded by the National Science Foundation (Collaborative Research Grants OCE-2032340 to MPH and OCE-2032340 to PAR).

References

Bach, L. T., & Boyd, P. W. (2021). Seeking natural analogs to fast-forward the assessment of marine CO_2 removal. *Proceedings of the National Academy of Sciences*, *118*(40), e2106147118. https://doi.org/10.1073/pnas.2106147118

Bereiter, B., Eggleston, S., Schmitt, J., Nehrbass-Ahles, C., Stocker, T. F., Fischer, H., et al. (2015). Revision of the EPICA Dome C CO_2 record from 800 to 600 kyr before present. *Geophysical Research Letters*, *42*(2), 542–549. https://doi.org/10.1002/2014GL061957

Bova, S. C., Herbert, T. D., & Altabet, M. A. (2018). Ventilation of northern and southern sources of aged carbon in the eastern equatorial Pacific during the younger Dryas rise in atmospheric CO_2. *Paleoceanography and Paleoclimatology*, *33*(11), 1151–1168. https://doi.org/10.1029/2018PA003386

Broecker, W. (2009). The mysterious ^{14}C decline. *Radiocarbon*, *51*(1), 109–119. https://doi.org/10.1017/S0033822200033737

Broecker, W., & Barker, S. (2007). A 190‰ drop in atmosphere's Δ14C during the "Mystery Interval" (17.5 to 14.5 kyr). *Earth and Planetary Science Letters*, *256*(1–2), 90–99. https://doi.org/10.1016/j.epsl.2007.01.015

Bryan, S. P., Marchitto, T. M., & Lehman, S. J. (2010). The release of 14C-depleted carbon from the deep ocean during the last deglaciation: Evidence from the Arabian Sea. *Earth and Planetary Science Letters*, *298*(1), 244–254. https://doi.org/10.1016/j.epsl.2010.08.025

Cartapanis, O., Galbraith, E. D., Bianchi, D., & Jaccard, S. L. (2018). Carbon burial in deep-sea sediment and implications for oceanic inventories of carbon and alkalinity over the last glacial cycle. *Climate of the Past*, *14*(11), 1819–1850. https://doi.org/10.5194/cp-14-1819-2018

Chalk, T. B., Hain, M. P., Foster, G. L., Rohling, E. J., Sexton, P. F., Badger, M. P. S., et al. (2017). Causes of ice age intensification across the Mid-Pleistocene Transition. *Proceedings of the National Academy of Sciences*, *114*(50), 13114–13119. https://doi.org/10.1073/pnas.1702143114

Chen, T., Robinson, L. F., Burke, A., Claxton, L., Hain, M. P., Li, T., et al. (2020). Persistently well-ventilated intermediate-depth ocean through the last deglaciation. *Nature Geoscience*, *13*(11), 733–738. Article 11. https://doi.org/10.1038/s41561-020-0638-6

De Pol-Holz, R., Keigwin, L., Southon, J., Hebbeln, D., & Mohtadi, M. (2010). No signature of abyssal carbon in intermediate waters off Chile during deglaciation. *Nature Geoscience*, *3*(3), 192–195. Article 3. https://doi.org/10.1038/ngeo745

Dinauer, A., Adolphi, F., & Joos, F. (2020). Mysteriously high Δ14C of the glacial atmosphere: Influence of 14C production and carbon cycle changes. *Climate of the Past*, *16*(4), 1159–1185. https://doi.org/10.5194/cp-16-1159-2020

Gehrie, E., Archer, D., Emerson, S., Stump, C., & Henning, C. (2006). Subsurface ocean argon disequilibrium reveals the equatorial Pacific shadow zone. *Geophysical Research Letters*, *33*(18). https://doi.org/10.1029/2006GL026935

Green, R. A. (2023). RyanAGreen/Deglacial-Neutralized-Carbon-14C: Submission to GRL (v1.0.0) [Dataset]. *Zenodo*. https://doi.org/10.5281/zenodo.7847185

Hain, M. P., Foster, G. L., & Chalk, T. (2018). Robust constraints on past CO_2 climate forcing from the boron isotope proxy. *Paleoceanography and Paleoclimatology*, *33*(10), 1099–1115. https://doi.org/10.1029/2018pa003362

Hain, M. P., Sigman, D. M., & Haug, G. H. (2010). Carbon dioxide effects of Antarctic stratification, North Atlantic Intermediate Water formation, and subantarctic nutrient drawdown during the last ice age: Diagnosis and synthesis in a geochemical box model. *Global Biogeochemical Cycles*, *24*(4). https://doi.org/10.1029/2010GB003790

Hain, M. P., Sigman, D. M., & Haug, G. H. (2011). Shortcomings of the isolated abyssal reservoir model for deglacial radiocarbon changes in the mid-depth Indo-Pacific Ocean. *Geophysical Research Letters*, *38*(4). https://doi.org/10.1029/2010GL046158

Hain, M. P., Sigman, D. M., & Haug, G. H. (2014). Distinct roles of the Southern Ocean and North Atlantic in the deglacial atmospheric radiocarbon decline. *Earth and Planetary Science Letters*, *394*, 198–208. https://doi.org/10.1016/j.epsl.2014.03.020

Hodell, D. A., Venz, K. A., Charles, C. D., & Ninnemann, U. S. (2003). Pleistocene vertical carbon isotope and carbonate gradients in the South Atlantic sector of the Southern Ocean. *Geochemistry, Geophysics, Geosystems*, *4*(1), 1–19. https://doi.org/10.1029/2002GC000367

Holzer, M., DeVries, T., & de Lavergne, C. (2021). Diffusion controls the ventilation of a Pacific Shadow Zone above abyssal overturning. *Nature Communications*, *12*(1), 4348. Article 1. https://doi.org/10.1038/s41467-021-24648-x

Huybers, P., & Langmuir, C. (2009). Feedback between deglaciation, volcanism, and atmospheric CO_2. *Earth and Planetary Science Letters*, *286*(3), 479–491. https://doi.org/10.1016/j.epsl.2009.07.014

Ito, T., & Follows, M. J. (2005). Preformed phosphate, soft tissue pump and atmospheric CO_2. *Journal of Marine Research*, *63*(4), 813–839. https://doi.org/10.1357/0022240054663231

Joos, F., Prentice, I. C., Sitch, S., Meyer, R., Hooss, G., Plattner, G.-K., et al. (2001). Global warming feedbacks on terrestrial carbon uptake under the Intergovernmental Panel on Climate Change (IPCC) emission scenarios. *Global Biogeochemical Cycles*, *15*(4), 891–907. https://doi.org/10.1029/2000GB001375

Keir, R. S. (1988). On the late Pleistocene ocean geochemistry and circulation. *Paleoceanography*, *3*(4), 413–445. https://doi.org/10.1029/PA003i004p00413

Khatiwala, S., Schmittner, A., & Muglia, J. (2019). Air-sea disequilibrium enhances ocean carbon storage during glacial periods. *Science Advances*, *5*(6), eaaw4981. https://doi.org/10.1126/sciadv.aaw4981

Köhler, P., Knorr, G., & Bard, E. (2014). Permafrost thawing as a possible source of abrupt carbon release at the onset of the Bølling/Allerød. *Nature Communications*, *5*(1), 5520. Article 1. https://doi.org/10.1038/ncomms6520

Lindsay, C. M., Lehman, S. J., Marchitto, T. M., Carriquiry, J. D., & Ortiz, J. D. (2016). New constraints on deglacial marine radiocarbon anomalies from a depth transect near Baja California. *Paleoceanography*, *31*(8), 1103–1116. https://doi.org/10.1002/2015PA002878

Lindsay, C. M., Lehman, S. J., Marchitto, T. M., & Ortiz, J. D. (2015). The surface expression of radiocarbon anomalies near Baja California during deglaciation. *Earth and Planetary Science Letters*, *422*, 67–74. https://doi.org/10.1016/j.epsl.2015.04.012

Marchitto, T. M., Lehman, S. J., Ortiz, J. D., Fluckiger, J., & van Geen, A. (2007). Marine radiocarbon evidence for the mechanism of deglacial atmospheric CO_2 rise. *Science*, *316*(5830), 1456–1459. https://doi.org/10.1126/science.1138679

Marcott, S. A., Bauska, T. K., Buizert, C., Steig, E. J., Rosen, J. L., Cuffey, K. M., et al. (2014). Centennial-scale changes in the global carbon cycle during the last deglaciation. *Nature*, *514*(7524), 616–619. Article 7524. https://doi.org/10.1038/nature13799

Margolskee, A., Frenzel, H., Emerson, S., & Deutsch, C. (2019). Ventilation pathways for the North Pacific oxygen deficient zone. *Global Biogeochemical Cycles*, *33*(7), 875–890. https://doi.org/10.1029/2018GB006149

Marinov, I., Follows, M., Gnanadesikan, A., Sarmiento, J. L., & Slater, R. D. (2008). How does ocean biology affect atmospheric pCO_2? Theory and models. *Journal of Geophysical Research*, *113*(C7). https://doi.org/10.1029/2007JC004598

Marinov, I., Gnanadesikan, A., Sarmiento, J. L., Toggweiler, J. R., Follows, M., & Mignone, B. K. (2008). Impact of oceanic circulation on biological carbon storage in the ocean and atmospheric pCO_2. *Global Biogeochemical Cycles*, *22*(3). https://doi.org/10.1029/2007GB002958

McManus, J. F., Francois, R., Gherardi, J.-M., Keigwin, L. D., & Brown-Leger, S. (2004). Collapse and rapid resumption of Atlantic meridional circulation linked to deglacial climate changes. *Nature*, *428*(6985), 834–837. Article 6985. https://doi.org/10.1038/nature02494

NASEM. (2021). *A research strategy for Ocean-based carbon dioxide removal and sequestration*. National Academies Press. https://doi.org/10.17226/26278

Ortiz, J. D., O'Connell, S. B., DelViscio, J., Dean, W., Carriquiry, J. D., Marchitto, T., et al. (2004). Enhanced marine productivity off western North America during warm climate intervals of the past 52 k.y. *Geology*, *32*(6), 521. https://doi.org/10.1130/G20234.1

Poggemann, D.-W., Nürnberg, D., Hathorne, E. C., Frank, M., Rath, W., Reißig, S., & Bahr, A. (2018). Deglacial heat uptake by the Southern Ocean and rapid northward redistribution via Antarctic Intermediate Water. *Paleoceanography and Paleoclimatology*, *33*(11), 1292–1305. https://doi.org/10.1029/2017PA003284

Pollack, H. N., Hurter, S. J., & Johnson, J. R. (1993). Heat flow from the Earth's interior: Analysis of the global data set. *Reviews of Geophysics*, *31*(3), 267–280. https://doi.org/10.1029/93RG01249

Rafter, P. A., Carriquiry, J. D., Herguera, J., Hain, M. P., Solomon, E. A., & Southon, J. R. (2019). Anomalous > 2000-year-old surface ocean radiocarbon age as evidence for deglacial geologic carbon release. *Geophysical Research Letters*, *46*(23), 13950–13960. https://doi.org/10.1029/2019GL085102

Rafter, P. A., Gray, W. R., Hines, S. K. V., Burke, A., Costa, K. M., Gottschalk, J., et al. (2022). Global reorganization of deep-sea circulation and carbon storage after the last ice age. *Science Advances*, *8*(46), eabq5434. https://doi.org/10.1126/sciadv.abq5434

Rafter, P. A., Herguera, J.-C., & Southon, J. R. (2018). Extreme lowering of deglacial seawater radiocarbon recorded by both epifaunal and infaunal benthic foraminifera in a wood-dated sediment core. *Climate of the Past*, *14*(12), 1977–1989. https://doi.org/10.5194/cp-14-1977-2018

Reimer, P. J., Austin, W. E. N., Bard, E., Bayliss, A., Blackwell, P. G., Ramsey, C. B., et al. (2020). The IntCal20 northern Hemisphere radiocarbon age calibration curve (0–55 cal kBP). *Radiocarbon*, *62*(4), 725–757. https://doi.org/10.1017/RDC.2020.41

Ronge, T. A., Tiedemann, R., Lamy, F., Köhler, P., Alloway, B. V., De Pol-Holz, R., et al. (2016). Radiocarbon constraints on the extent and evolution of the South Pacific glacial carbon pool. *Nature Communications*, *7*(1), 11487. https://doi.org/10.1038/ncomms11487

Rose, K. A., Sikes, E. L., Guilderson, T. P., Shane, P., Hill, T. M., Zahn, R., & Spero, H. J. (2010). Upper-ocean-to-atmosphere radiocarbon offsets imply fast deglacial carbon dioxide release. *Nature*, *466*(7310), 1093–1097. Article 7310. https://doi.org/10.1038/nature09288

Roth, R., & Joos, F. (2012). Model limits on the role of volcanic carbon emissions in regulating glacial–interglacial CO_2 variations. *Earth and Planetary Science Letters*, *329–330*, 141–149. https://doi.org/10.1016/j.epsl.2012.02.019

Roth, R., & Joos, F. (2013). A reconstruction of radiocarbon production and total solar irradiance from the Holocene ^{14}C and CO_2 records: Implications of data and model uncertainties. *Climate of the Past*, *9*(4), 1879–1909. https://doi.org/10.5194/cp-9-1879-2013

Shakun, J. D., Clark, P. U., He, F., Marcott, S. A., Mix, A. C., Liu, Z., et al. (2012). Global warming preceded by increasing carbon dioxide concentrations during the last deglaciation. *Nature*, *484*(7392), 49–54. Article 7392. https://doi.org/10.1038/nature10915

Siani, G., Michel, E., De Pol-Holz, R., DeVries, T., Lamy, F., Carel, M., et al. (2013). Carbon isotope records reveal precise timing of enhanced Southern Ocean upwelling during the last deglaciation. *Nature Communications*, *4*(1), 2758. Article 1. https://doi.org/10.1038/ncomms3758

Siegenthaler, U., Stocker, T. F., Monnin, E., Lüthi, D., Schwander, J., Stauffer, B., et al. (2005). Stable carbon cycle–climate relationship during the late Pleistocene. *Science*, *310*(5752), 1313–1317. https://doi.org/10.1126/science.1120130

Sigman, D. M., Fripiat, F., Studer, A. S., Kemeny, P. C., Martínez-García, A., Hain, M. P., et al. (2021). The Southern Ocean during the ice ages: A review of the Antarctic surface isolation hypothesis, with comparison to the North Pacific. *Quaternary Science Reviews*, *254*, 106732. https://doi.org/10.1016/j.quascirev.2020.106732

Sigman, D. M., Hain, M. P., & Haug, G. H. (2010). The polar ocean and glacial cycles in atmospheric CO_2 concentration. *Nature*, *466*(7302), 47–55. https://doi.org/10.1038/nature09149

Sigman, D. M., & Haug, G. H. (2003). The biological pump in the past. https://doi.org/10.1016/B0-08-043751-6/06118-1

Skinner, L. C., & Bard, E. (2022). Radiocarbon as a dating Tool and tracer in paleoceanography. *Reviews of Geophysics*, *60*(1), e2020RG000720. https://doi.org/10.1029/2020RG000720

Skinner, L. C., Fallon, S., Waelbroeck, C., Michel, E., & Barker, S. (2010). Ventilation of the deep Southern Ocean and deglacial CO2 rise. *Science*, *328*(5982), 1147–1151. https://doi.org/10.1126/science.1183627

Stott, L., Southon, J., Timmermann, A., & Koutavas, A. (2009). Radiocarbon age anomaly at intermediate water depth in the Pacific Ocean during the last deglaciation. *Paleoceanography*, *24*(2). https://doi.org/10.1029/2008PA001690

Stott, L., & Timmermann, A. (2011). Hypothesized link between glacial/interglacial atmospheric CO2 cycles and storage/release of CO_2-rich fluids from deep-sea sediments. In H. Rashid, L. Polyak, & E. Mosley-Thompson (Eds.), *Geophysical monograph series* (Vol. 193, pp. 123–138). American Geophysical Union. https://doi.org/10.1029/2010GM001052

Stott, L., Davy, B., Shao, J., Coffin, R., Pecher, I., Neil, H., et al. (2019). CO_2 release from pockmarks on the Chatham rise-bounty trough at the glacial termination. *Paleoceanography and Paleoclimatology*, *34*(11), 1726–1743. https://doi.org/10.1029/2019PA003674

Stott, L. D., Harazin, K. M., & Krupinski, N. B. Q. (2019). Hydrothermal carbon release to the ocean and atmosphere from the eastern equatorial Pacific during the last glacial termination. *Environmental Research Letters*, *14*(2), 025007. https://doi.org/10.1088/1748-9326/aafe28

Stuiver, M., & Polach, H. A. (1977). Discussion reporting of 14C data. *Radiocarbon*, *19*(3), 355–363. https://doi.org/10.1017/S0033822200003672

Yu, J., Anderson, R. F., Jin, Z., Rae, J. W. B., Opdyke, B. N., & Eggins, S. M. (2013). Responses of the deep ocean carbonate system to carbon reorganization during the Last Glacial–interglacial cycle. *Quaternary Science Reviews*, *76*, 39–52. https://doi.org/10.1016/j.quascirev.2013.06.020

Yu, J., Broecker, W. S., Elderfield, H., Jin, Z., McManus, J., & Zhang, F. (2010). Loss of carbon from the deep sea since the last glacial maximum. *Science*, *330*(6007), 1084–1087. https://doi.org/10.1126/science.1193221

Yu, J., Elderfield, H., & Piotrowski, A. M. (2008). Seawater carbonate ion-δ13C systematics and application to glacial–interglacial North Atlantic ocean circulation. *Earth and Planetary Science Letters*, *271*(1), 209–220. https://doi.org/10.1016/j.epsl.2008.04.010

Zhao, N., & Keigwin, L. D. (2018). An atmospheric chronology for the glacial-deglacial Eastern Equatorial Pacific. *Nature Communications*, *9*(1), 3077. Article 1. https://doi.org/10.1038/s41467-018-05574-x

Zhao, N., Marchal, O., Keigwin, L., Amrhein, D., & Gebbie, G. (2018). A synthesis of deglacial deep-sea radiocarbon records and their (in) consistency with modern ocean ventilation. *Paleoceanography and Paleoclimatology*, *33*(2), 128–151. https://doi.org/10.1002/2017pa003174

References From the Supporting Information

Bard, E. (1998). Geochemical and geophysical implications of the radiocarbon calibration. *Geochimica et Cosmochimica Acta*, *62*(12), 2025–2038. https://doi.org/10.1016/S0016-7037(98)00130-6

Galbraith, E. D., Kwon, E. Y., Bianchi, D., Hain, M. P., & Sarmiento, J. L. (2015). The impact of atmospheric pCO_2 on carbon isotope ratios of the atmosphere and ocean. *Global Biogeochemical Cycles*, *29*(3), 307–324. https://doi.org/10.1002/2014GB004929

Kovaltsov, G. A., Mishev, A., & Usoskin, I. G. (2012). A new model of cosmogenic production of radiocarbon 14C in the atmosphere. *Earth and Planetary Science Letters*, *337*(338), 114–120. https://doi.org/10.1016/j.epsl.2012.05.036

Laj, C., Kissel, C., & Beer, J. (2004). *High resolution global paleointensity stack since 75 kyr (GLOPIS-75) calibrated to absolute values* (Vol. 145, pp. 255–265). Washington DC American Geophysical Union Geophysical Monograph Series. https://doi.org/10.1029/145GM19

Mackensen, A., & Schmiedl, G. (2019). Stable carbon isotopes in paleoceanography: Atmosphere, oceans, and sediments. *Earth-Science Reviews*, *197*, 102893. https://doi.org/10.1016/j.earscirev.2019.102893

Press, W. H., Teukolsky, S. A., Vetterling, W. T., & Flannery, B. P. (2007). *Numerical recipes 3rd edition: The art of scientific computing*. Cambridge University Press.

Reimer, P. J., Bard, E., Bayliss, A., Beck, J. W., Blackwell, P. G., Ramsey, C. B., et al. (2013). IntCal13 and Marine13 radiocarbon age calibration curves 0–50,000 years cal BP. *Radiocarbon*, *55*(4), 1869–1887. https://doi.org/10.2458/azu_js_rc.55.16947